J|A|C|S ARTICLES

Published on Web 12/31/2009

Chemical Control of the Photoluminescence of CdSe Quantum Dot−Organic Complexes with a Series of Para-Substituted Aniline Ligands

Kathryn E. Knowles, Daniel B. Tice, Eric A. McArthur, Gemma C. Solomon, and Emily A. Weiss*

Department of Chemistry, Northwestern University, 2145 Sheridan Road, Evanston, Illinois 60208-3113

Received August 27, 2009; E-mail: e-weiss@northwestern.edu

Abstract: Replacement of the native (as-synthesized) ligands of colloidal CdSe QDs with varying concentrations of a series of para-substituted anilines (R-An), where R ranges from strongly electron-withdrawing to strongly electron-donating, decreases the PL of the QDs. The molar ratio of R-An to QD ([R-An]:[QD]) at which the PL decreases by 50% shifts by 4 orders of magnitude over the series R-An. The model employed to describe the data combines a Freundlich binding isotherm (which reflects the dependence of the binding affinity of the amine headgroups of R-An on the substituent R) with a function that describes the response of the PL to R-An ligands once they are bound at their equilibrium surface coverage. The latter function includes as a parameter the rate constant, k_{nr}, for nonradiative decay of the exciton at a site to which an R-An ligand is coordinated. The value of this parameter reveals that the predominant mechanism of QD−ligand interaction is passivation of Cd^{2+} surface sites through σ-donation for R-An ligands with R = H, Br, OCF_3, and reductive quenching through photoinduced hole transfer for R = MeO, $(Me)_2N$.

Introduction

This paper describes the mechanisms by which the chemical properties of a series of para-substituted anilines (R-An), with substituents (R) that range from strongly electron-withdrawing to strongly electron-donating (Chart 1), control the degree to which the R-An ligands decrease the photoluminescence (PL) of the colloidal CdSe quantum dots (QDs) to which they coordinate. We introduce the anilines to 2.9-nm QDs, which are initially passivated by a monolayer of long-chain alkyl phosphine oxides, alkylphosphonates, and amines (so-called "native" ligands),[1,2] through a solution-phase ligand exchange procedure, and record the PL of the solution as a function of the molar ratio of aniline to QD ([R-An]:[QD]). The concentration of added R-An ligand necessary to quench the PL of the solution of QDs by 50% shifts by 4 orders of magnitude over the series R-An. The observed dependence of PL on [R-An]:[QD] requires a model that includes two functions: a binding isotherm, and a function that describes the response of the PL to R-An ligands once they are bound at their equilibrium surface coverage;[3] both functions are sensitive to R. We use this model, along with independently estimated equilibrium constants for the binding of R-An to Cd^{2+}, to deconvolute the overall response of the PL into contributions from the binding affinity of the R-An ligands, and contributions from their electronic interactions with the surface once bound. The values of the rate constant, k_{nr}, for nonradiative decay of the excited state of the QD extracted from the model indicate that the R-An ligands separate into two groups based on the nature of their electronic interaction with the surfaces of the QDs: those ligands where R is electron-withdrawing act as weak passivators of Cd^{2+} surface sites,[4] and those ligands where R is electron-donating are active quenchers of the QDs. Oxidation potentials of the active quenchers suggest that the active quenching mechanism is photoinduced hole transfer from the QD exciton to the R-An ligand.

Chart 1. Structures of Para-Substituted Anilines, and Abbreviations Used in the Text

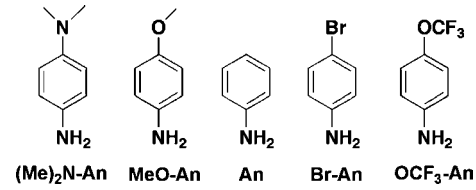

Background. The Surface Chemistry of CdSe QDs. Quantum dots are crystalline clusters of atoms with diameters on the order of the size of the exciton in the corresponding bulk semiconductor material (6 nm for CdSe).[5−8] An exciton is a net neutral pair of charge carriers resulting from photoexcitation: an electron in the conduction band and a positively charged "hole" in the valence band. Excitons within QDs experience spatial confine-

(1) Kopping, J. T.; Patten, T. E. *J. Am. Chem. Soc.* **2008**, *130*, 5689–5698.
(2) Kuno, M. L., J. K.; Dabbousi, B. O.; Mikulec, F. V.; Bawendi, M. G. *J. Chem. Phys.* **1997**, *106*, 9869–9882.
(3) Koole, R.; Schapotschnikow, P.; de Mello Donega, C.; Vlugt, T. J. H.; Meijerink, A. *ACS Nano* **2008**, *2*, 1703–1714.
(4) Nose, K.; Fujita, H.; Omata, T.; Otsuka-Yao-Matsuo, S.; Nakamura, H.; Maeda, H. *J. Lumin.* **2007**, *127*, 21–26.
(5) Klimov, V. I. *J. Phys. Chem. B* **2006**, *110*, 16827–16845.
(6) Murray, C. B.; Kagan, C. R.; Bawendi, M. G. *Annu. Rev. Mater. Sci.* **2000**, *30*, 545–610.
(7) Brus, L. E. *Proc. SPIE-Int. Soc. Opt. Eng.* **1994**, *2125*, 381–385.
(8) Garrett, M.; Bowers, M. J.; McBride, J. R.; Orndorff, R. L.; Pennycook, S. J.; Rosenthal, S. J. *J. Phys. Chem. C* **2008**, *112*, 436–442.

ment, which leads to concentration of the continuous energy spectrum of a bulk semiconductor into a set of high-oscillator-strength discrete transitions. We therefore refer, throughout this manuscript, to the electronic states that define the bandgap of the QD as the HOMO and LUMO.[9]

In small nanocrystals, a high percentage of the atoms interact with the surrounding medium;[8] for example, approximately 56% of the atoms in a 3-nm QD are at the surface.[6,10] In the absence of an inorganic shell comprising a higher-bandgap semiconductor, the dynamics of a spatially confined exciton in the QD are sensitive to the surface chemistry of the QDs. As evidenced by the sensitivity of the optical properties of QDs—the lifetime of the exciton, the quantum yield of PL, and the tendency to blink or photoionize—to the dielectric environment and to the material used to cap the surface of the QD, the exciton quickly delocalizes over both the core and surface. This delocalization is due especially to the contribution of the electron to the excitonic wave function.[9,11−21] Upon delocalization, the pathway by which the exciton decays is dictated by two factors: (i) the relative populations of different types of surface sites, and (ii) the relative rate constants for the decay processes associated with each type of site. Both of these factors can be controlled by coordination of organic ligands to the surfaces of the QDs. The ligands serve to prevent aggregation of the QDs and donate electrons to, or accept electrons from, dangling bonds of incompletely coordinated metal ions—Cd^{2+} sites are electron acceptors, Se^{2-} sites are electron donors—in order to preserve the core character of the nanocrystal.[4,11,22,23] The properties of coordinated ligands determine whether surface states will be located energetically near or within the bandgap of the QD and therefore serve as traps for charge carriers.[11,24−26] By synthetically altering organic ligands, we can, in principle, control the relative rates of processes that originate from excitonic states and therefore influence important observable properties of the QD such as its quantum yield of PL[22] and its yield of electron and hole transfer to acceptor moieties.[27,28]

The Importance of Studying QD−Organic Interfaces. Colloidal QD−organic complexes, because they form an optically clear suspension in many solvents, provide an opportunity to characterize organic/semiconductor interfaces with high signal-to-noise solution-phase spectroscopic methods rather than relying on traditional surface science techniques. Although these nanoscopic complexes have surfaces with a high radius of curvature that differ in structure from macroscopic surfaces, the results of studies on passivation and interfacial charge transfer in colloidal model systems can serve as a starting point for studies of planar interfaces.[29] Colloidal QDs also have a range of potential applications; they are efficient harvesters of UV, visible, and infrared light[6,30] and have the photostability and multiply degenerate states of a semiconductor[31] and the solution-processability and synthetic tunability of an organic molecule.[6] These properties, in addition to their ability to act as charge transfer partners for a variety of conjugated molecules and polymers,[32−36] make QDs suitable as active materials within hybrid organic−inorganic solar cells.[37−39] In order to function as a photovoltaic active material, however, QDs must be able to exchange charge carriers (electrons or holes), created either by photoexcitation or injection, with proximate QDs or with complementary active materials. This process is inhibited by states on the surface that thermodynamically and kinetically trap charge carriers and decrease the conductivity of even well-ordered films of QDs.[40−42] Many common ligands for QDs, such as the native ligands in this study—hexadecylamine (HDA), trioctylphosphine (TOP), and trioctylphosphine oxide (TOPO)—act as insulating tunneling barriers between QDs in the solid state and therefore are not appropriate ligands for forming electrically conductive films.[43−46] In this work, we explore the surface states created by short, conjugated ligands with tunable electronic properties: specifically, para-substituted anilines.

(9) Wang, Y.; Herron, N. *J. Phys. Chem.* **1991**, *95*, 525–532.
(10) Bischof, T.; Ivanda, M.; Lermann, G.; Materny, A.; Kiefer, W.; Kalus, J. *J. Raman Spectrosc.* **1996**, *27*, 297–302.
(11) Klimov, V. I.; McBranch, D. W.; Leatherdale, C. A.; Bawendi, M. G. *Phys. Rev. B: Condens. Matter Mater. Phys.* **1999**, *60*, 13740–13749.
(12) Banyai, L.; Gillot, P.; Hu, Y. Z.; Koch, S. W. *Phys. Rev. B: Condens. Matter Mater. Phys.* **1992**, *45*, 14136–14142.
(13) Blaudeck, T.; Zenkevich, E. I.; Cichos, F.; Von Borczyskowski, C. *J. Phys. Chem. C* **2008**, *112*, 20251–20257.
(14) Hill, N. A.; Whaley, K. B. *J. Chem. Phys.* **1994**, *100*, 2831–2837.
(15) Hollingsworth, J. A.; Vela, J.; Chen, Y.; Htoon, H.; Klimov, V. I.; Casson, R. *Proc. SPIE-Int. Soc. Opt. Eng.* **2009**, *7189*, 718904/1–718904/7.
(16) Li, S.; Steigerwald, M. L.; Brus, L. E. *ACS Nano* **2009**, *3*, 1267–1273.
(17) Wang, X.; Ren, X.; Kahen, K.; Hahn, M. A.; Rajeswaran, M.; Maccagnano-Zacher, S.; Silcox, J.; Cragg, G. E.; Efros, A. L.; Krauss, T. D. *Nature* **2009**, *459*, 686–689.
(18) Kovalevskij, V.; Gulbinas, V.; Piskarskas, A.; Hines, M. A.; Scholes, G. D. *Phys. Status Solidi B* **2004**, *241*, 1986–1993.
(19) Bawendi, M. G.; Carroll, P. J.; Wilson, W. L.; Brus, L. E. *J. Chem. Phys.* **1992**, *96*, 946–954.
(20) Pokrant, S.; Whaley, K. B. *Eur. Phys. J. D* **1999**, *6*, 255–267.
(21) Peterson, J. J.; Krauss, T. D. *Phys. Chem. Chem. Phys.* **2006**, *8*, 3851–3856.
(22) Issac, A.; von Borczyskowski, C.; Chichos, F. *Phys. Rev. B* **2005**, *71*, 161302/1–161302/4.
(23) Chowdhury, P. S.; Ghosh, P.; Patra, A. *J. Lumin.* **2007**, *124*, 327–332.
(24) Kalyuzhny, G.; Murray, R. W. *J. Phys. Chem. B* **2005**, *109*, 7012–7021.
(25) Munro, A. M.; Ginger, D. S. *Nano Lett.* **2008**, *8*, 2585–2590.
(26) Jarosz, M. V.; Stott, N. E.; Drndic, M.; Morgan, N. Y.; Kastner, M. A.; Bawendi, M. G. *J. Phys. Chem. B* **2003**, *107*, 12585–12588.
(27) Anderson, N. A.; Lian, T. *Annu. Rev. Phys. Chem.* **2005**, *56*, 491–519.
(28) Dibbell, R. S.; Watson, D. F. *J. Phys. Chem. C* **2009**, *113*, 3139–3149.
(29) Rajh, T.; Micic, O. I.; Lawless, D.; Serpone, N. *J. Phys. Chem.* **1992**, *96*, 4633–4641.
(30) Yun, D.; Feng, W.; Wu, H.; Yoshino, K. *Sol. Energy Mater. Sol. Cells* **2009**, *93*, 1208–1213.
(31) Ellis, A. B.; Brainard, R. J.; Kepler, K. D.; Moore, D. E.; Winder, E. J.; Kuech, T. F. *J. Chem. Educ.* **1997**, *74*, 680–684.
(32) Qi, D.; Fischbein, M.; Drndic, M.; Selmic, S. *Appl. Phys. Lett.* **2005**, *86*, 093103/1–093103/3.
(33) Sun, B.; Marx, E.; Greenham, N. C. *Nano Lett.* **2003**, *3*, 961–963.
(34) Sharma, S. N.; Pillai, Z. S.; Kamat, P. V. *J. Phys. Chem. B* **2003**, *107*, 10088–10093.
(35) Greenham, N. C.; Peng, X.; Alivisatos, A. P. *Phys. Rev. B* **1996**, *54*, 17628–17637.
(36) Ginger, D. S.; Greenham, N. C. *Phys. Rev. B* **1999**, *59*, 10622–10629.
(37) Lewis, N. S. *Inorg. Chem.* **2005**, *44*, 6900–6911.
(38) Dennler, G.; Scharber, M. C.; Ameri, T.; Denk, P.; Forberich, K.; Waldauf, C.; Brabec, C. J. *Adv. Mater.* **2008**, *20*, 579–583.
(39) Kippelen, B.; Bredas, J. L. *Energy Environ. Sci.* **2009**, *2*, 251–261.
(40) Jones, M.; Lo, S. S.; Scholes, G. D. *Proc. Natl. Acad. Sci. U.S.A.* **2009**, *106*, 3011–3016.
(41) Bryant, G. W.; Jaskolski, W. *J. Phys. Chem. B* **2005**, *109*, 19650–19656.
(42) Dayal, S.; Burda, C. *J. Am. Chem. Soc.* **2007**, *129*, 7977–7981.
(43) Talapin, D. V.; Murray, C. B. *Science* **2005**, *310*, 86–89.
(44) Mattoussi, H.; Cumming, A. W.; Murray, C. B.; Bawendi, M. G.; Ober, R. *Phys. Rev. B* **1998**, *58*, 7850–7863.
(45) Yu, D.; Wehrenberg, B. L.; Jha, P.; Ma, J.; Guyot-Sionnest, P. *J. Appl. Phys.* **2006**, *99*, 104315/1–104315/7.
(46) Jarosz, M. V.; Porter, V. J.; Fisher, B. R.; Kastner, M. A.; Bawendi, M. G. *Phys. Rev. B* **2004**, *70*, 195327/1–195327/12.

Experimental Strategy. Several groups have reported the response of PL of QDs exposed to ligands with thiol, amine, and phosphonic acid headgroups.[3,24,47−49] These studies, however, used series of ligands that varied by more than one structural component. Our strategy allows us to isolate the influence of the para substituent in a series of aniline derivatives by keeping all other variables in the system, such as the chemical structure of the headgroup and conjugated core of the ligands, the volume occupied by the ligands, and the initial surface coverage of the QDs, which determines their initial quantum yield of PL, approximately constant. We chose para-substituted anilines because of the well-established links between the substituents and the electronic properties of the molecules.[50,51] We show that, even for this limited series of ligands, there exists more than one mechanism by which the PL depends on the electronic substituent, R. Our results highlight the importance of using well-controlled, systematic variations in the structure of ligands[52,53] when determining how surface chemistry influences the optical and electronic properties of QDs.

Experimental Methods

Synthesis and Purification of CdSe QDs. We synthesized colloidal CdSe QDs using the organometallic precursor-based procedure of Qu et al. with minor modifications (see Supporting Information).[54] We arrested the growth of the QDs after injection of the Se precursor, TOPSe, which was prepared and stored in a glovebox, by quickly cooling the reaction with 10 mL of hexanes, and then allowed the resulting solution to stand for 12 h in the dark, during which time a white precipitate (excess cadmium stearate, TOPO, and HDA) formed. Centrifugation of this suspension (at 3500 rpm for 5 min) separated the white pellet, which we discarded, from a red supernate that contained the QDs. Addition of methanol to the supernate (1:1 by volume) and further centrifugation produced a red pellet of QDs and a colorless supernate containing HDA and TOPO. We discarded the supernate, dried the QD pellet with a stream of nitrogen, and stored it in the dark under a nitrogen atmosphere until use. The ground-state absorption spectrum of the QDs in distilled $CHCl_3$, Figure 1A, contains a peak at 540 nm assigned to the band-edge transition (HOMO to LUMO). According to previous work,[55] this energy corresponds to QDs with a diameter of 2.9 nm. The PL spectrum of the QDs, also in distilled $CHCl_3$, Figure 1A, shows a narrow (fwhm = 23 nm) emission peak centered at 550 nm, which indicates the QD sample has a monodispersity of 5−10%.[55,56] Analysis of the size distribution of QDs from a transmission electron micrograph, Figure 1B, also yields an average diameter of 2.9 nm ± 0.3 nm (see Supporting Information).

Ligand Exchange with R-An. We redispersed the QD pellet in freshly distilled $CHCl_3$[47] to a concentration of $5.1 \times 10^{-7} - 6.0 \times 10^{-7}$ M, as measured with ground-state absorption spectroscopy.[55]

(47) Munro, A. M.; Plante, I. J.-L.; Ng, M. S.; Ginger, D. S. *J. Phys. Chem. C* **2007**, *111*, 6220–6227.
(48) Ji, X.; Copenhaver, D.; Sichmeller, C.; Peng, X. *J. Am. Chem. Soc.* **2008**, *130*, 5726–5735.
(49) Bullen, C.; Mulvaney, P. *Langmuir* **2006**, *22*, 3007–3013.
(50) Gross, K. C.; Seybold, P. G. *Int. J. Quantum Chem.* **2000**, *80*, 1107–1115.
(51) Gross, K. C.; Seybold, P. G.; Hadad, C. M. *Int. J. Quantum Chem.* **2002**, *90*, 445–458.
(52) Murphy, C. J.; Lisensky, G. C.; Leung, L. K.; Kowach, G. R.; Ellis, A. B. *J. Am. Chem. Soc.* **1990**, *127*, 2752–2757.
(53) Guo, R. S., Y.; Wang, G. L.; Murray, R. W. *J. Am. Chem. Soc.* **2005**, *127*, 2752–2757.
(54) Qu, L. H.; Peng, X. G. *J. Am. Chem. Soc.* **2002**, *124*, 2049–2055.
(55) Yu, W. W.; Qu, L. H.; Guo, W.; Peng, X. G. *Chem. Mater.* **2003**, *15*, 2854–2860.
(56) Steckel, J. S.; Zimmer, J. P.; Coe-Sullivan, S.; Stott, N. E.; Bulovic, V.; Bawendi, M. G. *Angew. Chem., Int. Ed. Engl.* **2004**, *43*, 2154–2158.

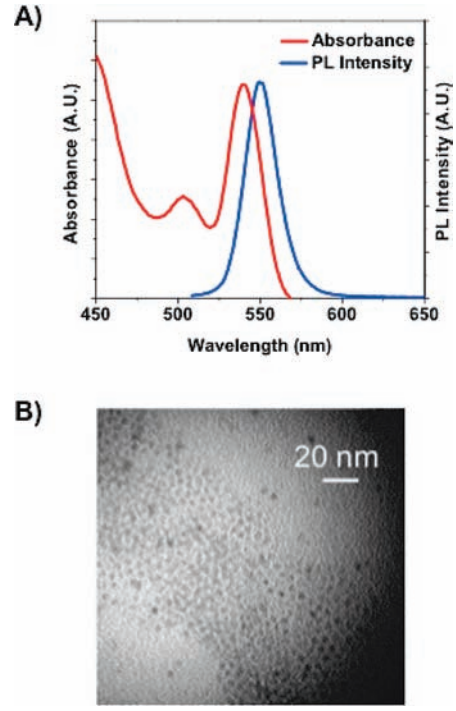

Figure 1. (A) Ground-state absorption (red) and PL (blue) spectra in distilled $CHCl_3$ of CdSe QDs used in the PL studies. The HOMO−LUMO absorption maximum is at 540 nm; this band gap is characteristic of QDs with a diameter of 2.9 nm. The data points in Figure 2 are the integrated intensities of the PL peak centered at 550 nm plotted against [R-An]:[QD]. The PL peak has a full width at half-maximum (fwhm) of 23 nm. (B) Transmission electron micrograph of QDs used in the PL intensity studies. The QDs exhibit a uniformly spherical shape with an average diameter of 2.9 nm ± 0.3 nm.

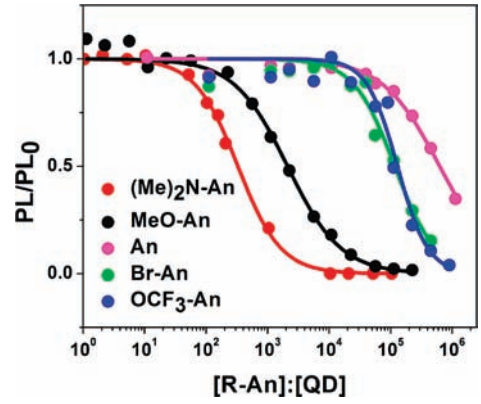

Figure 2. The ratio of the integrated PL intensity of QDs after stirring for 24 h in solutions of R-An and the integrated PL intensity of QDs before addition of anilines (PL_0), plotted against [R-An]:[QD]. Equations 3−7 derive and define the function used to fit these curves. The maximum and minimum values of PL/PL_0 are constrained to equal 1 and 0, respectively.

The QD solution was stirred under nitrogen atmosphere for three days so that the ligand-capped QDs reached equilibrium with the free native ligands, predominantly HDA, TOPO, and TOP.[3] In order to exchange native ligands with R-An ligands, we added 0.31 mL of an R-An solution of appropriate concentration in distilled $CHCl_3$ to 5 mL of QD solution so that the final mixtures had [R-An]:[QD] from 1:1 to 10^6:1. We stirred the solutions of QDs and R-An ligands in tightly capped vials under ambient atmosphere and in the dark for 24 h, at which point we knew that the solutions had come to equilibrium because their PL intensities had not changed for several hours (see Supporting Information). The substituted

anilines, *N,N*-dimethyl-*p*-phenylenediamine ($(Me)_2$N-An), *p*-anisidine (MeO-An), 4-bromoaniline (Br-An), and 4-(trifluoromethoxy)-aniline (OCF_3-An), were used as-received from Aldrich. We distilled aniline (An) (Aldrich) before use because, as-received, it was discolored.The Supporting Information contains ^{1}H NMR spectra of each of the R-An ligands. We detect 1−2% impurities in both unpurified substituted anilines and in the distilled unsubstituted aniline. During the ligand exchange process, the R-An molecules probably displace the native ligands in the order of increasing energy of adsorption on a CdSe surface: TOP (bound to Cd^{2+}, not to Se^{2-}) < TOPO, HDA < alkylphosphonates, where the alkylphosphonates are the deprotonated forms of the phosphonic acids (octylphosphonic acid and *P′*,*P′*-(di-*n*-octyl) dihydrogen pyrophosphonic acid) present as tight-binding impurities in reagent-grade TOPO.[1−3,57−59] Ground-state absorption spectra of the QDs before and after ligand exchange with R-An (at concentrations of R-An at which the PL of the sample decreases by 50%) show that the band-edge and higher-energy transitions do not shift upon coordination with R-An.

Steady-State PL of QDs Exposed to R-An Ligands. We excited the solutions of QDs and R-An ligands at 503 nm, the maximum of the second peak in the QD absorption spectrum, and recorded the PL intensity integrated over the entire PL peak of the QDs shown in Figure 1A. We did not excite the QDs at their band-edge (540 nm) because excitation at this wavelength would only allow us to observe the lower-energy portion of the PL peak. Figure 2 plots the final PL intensity divided by the PL intensity of the QD solution before addition of R-An ligands (PL/PL_0) versus the ratio of concentration of added R-An ligand to concentration of QDs ([R-An]:[QD]). The maximum value of [R-An]:[QD] was limited by the value of [R-An] that saturated the solution. We obtained the data for all of the R-An ligands except for $(Me)_2$N-An with QDs whose absorption and PL spectra are pictured in Figure 1. We used a separate batch of QDs (3.0 nm in diameter) for the ligand exchange reactions with $(Me)_2$N-An. Because of fluctuations in temperature during the synthesis, it is difficult to produce two batches of QDs of exactly the same size.[60]

Results and Discussion

Ligand Exchange with R-An Decreases the PL of the QDs with an Efficiency That Depends on R. Inspection of the data in Figure 2 shows that PL/PL_0 decreases with increasing [R-An]:[QD] with a shape that fits a sigmoidal function, which we derive in a subsequent section. The concentration of R-An ligand necessary to quench the PL of the solution of QDs depends on R and increases in the order: $(Me)_2$N-An < MeO-An < Br-An < OCF_3-An < An. We can separate the influence of the substituent, R, on the response of the PL of the QDs to the addition of R-An into two effects: (i) the effect of R on the affinity of R-An for binding to the surface of the QD, as given by the equilibrium constant for exchange with native ligand, X, $K_{Cd\text{-}QD}$, defined in eq 1, and (ii) the effect of R on the electronic interaction of R-An with the QD once it is

$$\text{R-An:QD} + \text{X} \overset{K_{Cd-QD}}{\rightleftharpoons} \text{R-An} + \text{QD:X},$$

$$K_{Cd\text{-}QD} = \frac{[\text{R-An}][\text{QD:X}]}{[\text{R-An:QD}][\text{X}]} \quad (1)$$

coordinated to the surface. We were not able to measure directly the values of $K_{Cd\text{-}QD}$, for a variety of reasons detailed in the Supporting Information. In principle, however, the R-An ligands with electron-donating substituents, $(Me)_2$N-An and MeO-An, which have amine groups with sp^3-like geometry, should bind more tightly than R-An ligands with the electron-withdrawing substituents, Br-An and OCF_3-An, which have amine groups with sp^2-like geometry.[50,61] The Supporting Information contains DFT-calculated geometries for the series R-An that support this trend. Furthermore, previous measurements[62] of the equilibrium constants for binding of R-An ligands to free Cd^{2+} ions, $K_{Cd\text{-}ion}$, showed that the strength of the interaction between Cd^{2+} ion and R-An increases as the electron-donating character of R increases, as given by the Hammett coefficient of R, Table 1.[63] We therefore used the experimentally measured values of $K_{Cd\text{-}ion}$ for An, MeO-An, and *p*-toluidine (Me-An)[62] and eq 2[64] to calculate the values of $K_{Cd\text{-}ion}$ for the

$$\log \frac{K_{Cd\text{-}ion}(\text{R})}{K_{Cd\text{-}ion}(\text{H})} = \rho\sigma \quad (2)$$

remaining R-An ligands in our study, Table 1, where $K_{Cd\text{-}ion}$(R) is the value of $K_{Cd\text{-}ion}$ for R-An, $K_{Cd\text{-}ion}$ (H) is the value of $K_{Cd\text{-}ion}$ for An, and ρ is the Hammett reaction constant (see Supporting Information). In eq 2, we used the Hammett coefficients, σ,[64] measured in cyclohexane, rather than in water, because our ligand exchange occurs in chloroform ($\varepsilon = 4.8$), and aqueous Hammett constants overestimate the basicities of the amine groups on the R-An ligands with electron-donating substituents in nonpolar solvents.[65] We then calculated the competitive binding constants[3] $K_{Cd\text{-}QD}$ (eq 1, Table 1) by dividing $K_{Cd\text{-}ion}$(R-An) by $K_{Cd\text{-}ion}$(HDA), which we approximated with the measured value for propylamine (0.0025). We believe that the ligand exchange process most relevant to the PL of the QDs is the competition between R-An and HDA for Cd^{2+} sites on the surfaces of the QDs because, as seen previously,[49] addition of HDA to CdSe QDs prepared identically to those used to acquire the data in Figure 2 increased the PL by a factor of 1.3, while addition of TOPO did not change their PL.

The values of $K_{Cd\text{-}QD}$ have a range of less than 1 order of magnitude over the series R. This result is not surprising, as ^{1}H NMR spectra of solutions of QDs and R-An ligands at various [R-An]:[QD] ratios (see Supporting Information) show that all of the R-An ligands have similar binding affinities for the QDs. As Murphy et al.[52] also found for the binding of a series of

(57) Puzder, A.; Williamson, A. J.; Zaitseva, N.; Galli, G.; Manna, L.; Alivisatos, A. P. *Nano Lett.* **2004**, *4*, 2361–2365.
(58) Rempel, J. Y.; Trout, B. L.; Bawendi, M. G.; Jensen, K. F. *J. Phys. Chem. B* **2006**, *110*, 18007–18016.
(59) Owen, J. S.; Park, J.; Trudeau, P.-E.; Alivisatos, A. P. *J. Am. Chem. Soc.* **2008**, *130*, 12279–12281.
(60) The data in Figure 2 is sensitive to the size of the QDs, but experiments with $(Me)_2$N-An:QD complexes show that a change in diameter of 0.1 nm shifts the plots in Figure 2 horizontally by less than a factor of two. This shift does not affect our interpretation of the data.
(61) Hoft, R. C. F., M. J.; McDonagh, A. M.; Cortie, M. B. *J. Phys. Chem. C* **2007**, *111*, 13886–13891.
(62) Martell, A. E.; Smith, R. M. *Critical Stability Constants*; Plenum Press: New York, 1974−1989; Vol. 2.
(63) All of the substituents in Table 1 donate electron density to the aromatic ring of the aniline via resonance interactions and withdraw via inductive interactions; however, the overall Hammett constants for $(Me)_2$N and MeO are negative (they are net electron donors), and those for Br and OCF_3 are positive (they are net electron withdrawers). Evidence for the relative contributions of resonance and inductive effects can be seen in the distribution of unpaired spin in the radical cations of R-An molecules (see Supporting Information).
(64) Anslyn, E. V.; Dougherty, D. A. *Modern Physical Organic Chemistry*; University Science Books: Sausalito, CA, 2006.
(65) Hansch, C.; Leo, A.; Taft, R. W. *Chem. Rev.* **1991**, *91*, 165–195.

Table 1. Hammett Para-Substituent Constants for Substituents R in Cyclohexane[a,b] and Values of $K_{Cd\text{-}ion}$ and $K_{Cd\text{-}QD}$ for the Corresponding Ligands R-An

	σ (c-C_6H_{12})[c]				
para-substituent (R)	σ	σ_I	σ_R	$K_{Cd\text{-}ion}$ (in H_2O)	$K_{Cd\text{-}QD}$ (in H_2O)[d]
$(Me)_2N$	−0.42	0.17	−0.56	0.34[e]	130
MeO	−0.40	0.30	−0.43	0.35[f]	160
H	0.00	0.00	0.00	0.79[f]	320
Br	0.27	0.49	−0.16	1.4[e]	500
OCF_3	0.37	0.62	−0.18	1.7[e]	630

[a] From ref 65. [b] σ_I = inductive contribution, σ_R = resonance contribution. [c] Calculated from ^{19}F NMR shifts of para-substituted fluorobenzenes. [d] Defined by equilibrium in eq 1, where $K_{Cd\text{-}QD} = K_{Cd\text{-}ion}(R\text{-}An)/K_{Cd\text{-}ion}(propylamine)$. [e] Calculated using the Hammett equation and values for $K_{Cd\text{-}ion}$ from reference 62. [f] From reference 62.

para-substituted anilines to a surface of bulk CdSe, the influence of the substituent R on the ability of R-An to quench the PL of the QDs in our study is much larger than that predicted solely by the range of equilibrium constants $K_{Cd\text{-}QD}$. If the *x*-coordinates of the plots in Figure 2 (at $PL/PL_0 = 0.5$, for instance) were dictated only by relative binding affinities, the range of these *x*-coordinates would be less than 1 order of magnitude over the series of R. We observe, however, that the *x*-coordinates have a range of *4 orders of magnitude*.[66] This observation strongly suggests that binding affinity is *not* the dominant factor in determining the influence of the substituent R on the PL of the QDs, and that, in order to model the data in Figure 2, we also need to consider the influence of R on the electronic interactions between a coordinated R-An ligand and the QD.

By using $K_{Cd\text{-}ion}$ to calculate $K_{Cd\text{-}QD}$, we probably underestimate the value of $K_{Cd\text{-}QD}$ because (i) theoretical calculations indicate[8−10] that the dissociation constant for complexes with cadmium ions localized on the surface of a QD is larger than that for complexes with free cadmium ions, and (ii) the binding of R-An ligands to the surface of CdSe is sterically hindered by the presence of the native long-chain alkylamines, trialkylphosphines and phosphine oxides, and octylphosphonic acid ligands already in equilibrium with the QDs. In using $K_{Cd\text{-}ion}$ to predict $K_{Cd\text{-}QD}$, we have also assumed that $K_{Cd\text{-}QD}$ is correlated with the Hammett coefficient of the substituent, R. We note that the Hammett analysis, although successful in predicting the relative binding affinities of para-substituted anilines to Cd^{2+} in solution, is not necessarily applicable to the binding equilibria of these ligands to surfaces of colloidal QDs. In colloid−ligand systems, the substituent R, in addition to influencing the basicity of the amine, could affect the probability of intermolecular interactions (possibly $\pi-\pi$ stacking) between ligands on the surface, and the ligands' response to changes in dielectric constant between bulk solvent and the immediate solvent shell of the QD. The validity of Hammett analysis in nanoparticle systems is supported, however, by its successful prediction of the trend in rate constants for exchange of native ligands for para-substituted arylthiols in gold nanoparticle systems.[67]

Figure 3 contains molecular orbital (MO) diagrams illustrating the electronic interactions between organic ligands and Cd^{2+} surface sites. In the absence of a ligand, an electron-poor Cd^{2+} surface site on a QD forms an electron-trapping surface state whose energy lies between the HOMO and LUMO of the core, which we approximate as the bonding and antibonding orbitals, respectively, of a Cd−Se bond (Figure 3A). Since the participating orbitals of Cd^{2+} have mostly 5s character,[68] they interact most strongly with σ-donating ligands, rather than π-bonding ligands, to form bonding and antibonding MOs. The relative energies of these MOs depend on the strength of the Cd^{2+}−ligand interaction, which depends on the σ-donating ability of the ligand as given by its electronegativity and basicity.[4,69] A strong σ-donating ligand interacts with Cd^{2+} to form an antibonding orbital with energy above that of the LUMO of the QD (Figure 3B) and effectively passivates the surface site by removing an electron-trapping midgap state. A weak σ-donor forms an antibonding orbital with energy below the LUMO of the QD (Figure 3C); this orbital can act as an electron trap. We show only Cd^{2+}−ligand interactions in Figure 3 for simplicity and also because we only perturb the system with ligands that bind to Cd^{2+} (σ-donors). The same principles apply to Se^{2-} sites, which have electron density available for bonding in their 4p orbitals[68] and will interact with σ- or π-accepting ligands rather than with σ-donors. Unpassivated Se^{2-} ions serve as trap sites for holes.[69]

In the model described below, we consider the R-An ligands to be weak σ-donors and the native ligands to be strong σ-donors; therefore, a well-passivated site is a site coordinated to a native ligand, such as HDA, and a poorly passivated site is a site coordinated to an R-An ligand.

The Model for PL/PL_0: A Binding Isotherm Combined with a Two-State Competitive Rate Model for the Decay of the Exciton. Consider an ensemble of QDs, where each QD in the ensemble can only exist in two states, emissive (the exciton decays with rate constant k_r) or nonemissive (the exciton decays with rate constant k_{nr}). The fraction of QDs in the ensemble that are emissive is equivalent to the probability that an average single QD within the ensemble is emissive—that is, the quantum yield of a single QD, Φ. A QD will be emissive if its exciton interacts with a surface state localized at a well-passivated site (Figure 3B) and will not be emissive if its exciton interacts with a surface state localized at a poorly passivated site (Figure 3C). The quantum yield of a QD, given by eq 3, is the ratio of τ_{obs}, the observed time constant

$$\Phi = \frac{\tau_{obs}}{\tau_r} = \frac{k_r}{(1-\theta)k_r + \theta k_{nr}} \tag{3}$$

for decay of the exciton, and $\tau_r = 1/k_r$, the time constant for decay that we would observe if every surface site on the QD were well-passivated. The observed time constant, τ_{obs}, is the reciprocal of the average of k_r and k_{nr}, weighted, respectively, by $(1-\theta)$, the fraction of well-passivated surface sites (those coordinated to HDA ligands), and θ, the fraction of poorly passivated surface sites (those coordinated to R-An ligands).

We assume that, prior to ligand exchange, the surfaces of the QDs are completely covered with native ligand, that is, $\theta = 0$, so the quantum yield of the QD before ligand exchange, Φ_0, is, in this model, unity. In reality, the initial quantum yield of the ensemble is not unity, because the QDs do contain empty and poorly passivated sites on the surface. The observable in this experiment, however, is the *decrease* in PL upon addition of R-An ligands, not the absolute value of this PL. After exchange, $(1-\theta)$ and θ are the equilibrium fractional surface

(66) The Supporting Information contains NMR spectra that show that the An ligand does not degrade during the process of ligand exchange.
(67) Donkers, R. L.; Song, Y.; Murray, R. W. *Langmuir* **2004**, *20*, 4703–4707.
(68) Albe, V.; Jouanin, C.; Bertho, D. *Phys. Rev. B: Condens. Matter Mater. Phys.* **1998**, *58*, 4713–4720.
(69) Guyot-Sionnest, P.; Shim, M.; Matranga, C.; Hines, M. *Phys. Rev. B: Condens. Matter Mater. Phys.* **1999**, *60*, R2181–R2184.

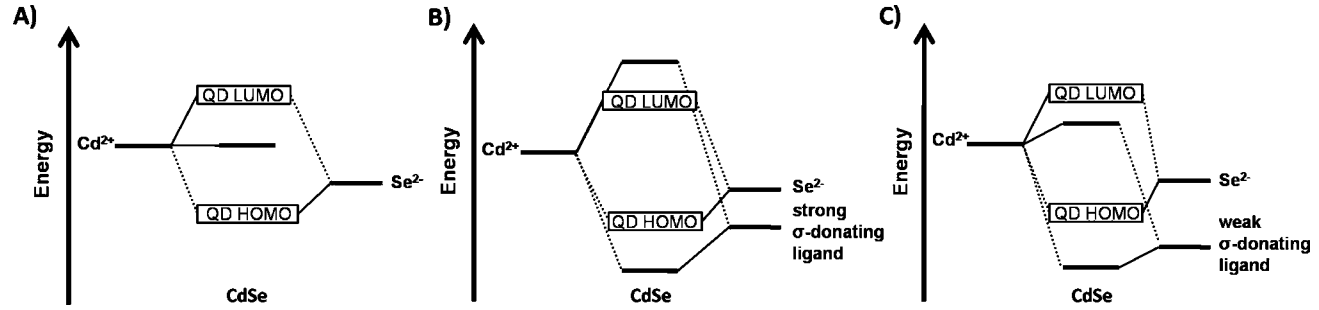

Figure 3. Qualitative molecular orbital diagrams describing bonding interactions between electron-poor Cd^{2+} surface sites on QDs and σ-donating ligands. (A) An empty Cd^{2+} surface site results in a state within the HOMO−LUMO gap that traps photoexcited electrons from the LUMO of the QD. (B) A strong σ-donating ligand eliminates the electron-trapping midgap state by binding to the Cd^{2+} site and forming an antibonding orbital that is higher in energy than the LUMO of the QD. The corresponding bonding orbital does not form a hole-trapping midgap state because it is lower in energy than the HOMO of the QD. (C) A weak σ-donating ligand increases the energy of the electron-trapping midgap state over that of bare Cd^{2+} but does not eliminate the trap because it forms an antibonding orbital that is lower in energy than the LUMO of the QD.

coverages of HDA and R-An ligand, respectively. Equation 4 is the resulting expression for the experimental

$$\frac{\mathrm{PL}}{\mathrm{PL}_0} = \frac{\Phi}{\Phi_0} = \frac{k_\mathrm{r}}{(1-\theta)k_\mathrm{r} + \theta k_\mathrm{nr}} \tag{4}$$

observable, $\mathrm{PL/PL_0}$. Rearrangement of the terms in eq 4 yields eq 5. We now choose to model θ

$$\frac{\mathrm{PL}}{\mathrm{PL}_0} = \frac{1}{1 + \theta(k_\mathrm{nr} - k_\mathrm{r})/k_\mathrm{r}} \tag{5}$$

with a Freundlich binding isotherm, which has successfully modeled the adsorption of organic molecules onto energetically and structurally heterogeneous surfaces, including nanocrystalline CdS films.[70] Although physically more straightforward to interpret, incorporation of the Langmuir isotherm[3,47−49] into eq 5 produced fitting parameters that exhibited an unacceptable level of codependence. Additionally, the Langmuir isotherm does not account for several nonidealities of the QD−organic system, as detailed in the Supporting Information. The form of the Freundlich isotherm is given in eq 6, where $K_\mathrm{Cd\text{-}QD}$ is the competitive dissociation constant for

$$\theta = \frac{1}{K_\mathrm{Cd-QD}}[\text{R-An}]^n \tag{6}$$

the R-An:QD complex, as defined in eq 1, and n is a fitting parameter that corresponds to the steepness of the decrease of $\mathrm{PL/PL_0}$ with increasing [R-An].[71] Substitution of eq 6 into eq 5 yields eqs 7a and 7b, which we use to fit plots of $\mathrm{PL/PL_0}$ vs the absolute concentration [R-An]

$$\frac{\mathrm{PL}}{\mathrm{PL}_0} = \frac{1}{1 + (K_\mathrm{Cd-QD})^{-1}[\text{R-An}]^n \dfrac{k_\mathrm{nr} - k_\mathrm{r}}{k_\mathrm{r}}} = \frac{1}{1 + C[\text{R-An}]^n} \tag{7a}$$

$$C = \frac{1}{K_\mathrm{Cd-QD}} \frac{k_\mathrm{nr} - k_\mathrm{r}}{k_\mathrm{r}} \tag{7b}$$

(the Supporting Information contains these plots). Figure 2 plots $\mathrm{PL/PL_0}$ vs the more physically intuitive variable, [R-An]:[QD]. Table 2 lists the values of the fitting parameters, C and n, for each R-An. When we multiply C by $K_\mathrm{Cd\text{-}QD}$, we obtain a set of values for $(k_\mathrm{nr} - k_\mathrm{r})/k_\mathrm{r}$ for the R-An ligands. The value of k_r is independent of R-An, so we have the trend $k_\mathrm{nr}((\mathrm{Me})_2\text{N-An}) > k_\mathrm{nr}(\text{MeO-An}) > k_\mathrm{nr}(\mathrm{OCF_3}\text{-An}) > k_\mathrm{nr}(\text{Br-An}) > k_\mathrm{nr}(\text{An})$. This trend in k_nr is what remains when we remove the contribution of binding affinity from the overall PL response.

Table 2. Values of the Parameters Obtained from Fitting $\mathrm{PL/PL_0}$ vs [R-An] to eq 7a

ligand	C^a	n^a	$(k_\mathrm{nr} - k_\mathrm{r})/k_\mathrm{r}{}^{a,b}$
$(\mathrm{Me})_2$N-An	5.3×10^4	1.2	6.6×10^6
MeO-An	9.6×10^2	1.0	1.5×10^5
An	2.7×10^0	0.90	8.5×10^2
Br-An	4.1×10^1	1.3	2.1×10^4
$\mathrm{OCF_3}$-An	1.6×10^2	1.9	8.6×10^4

[a] These parameters are unitless by definition. [b] Calculated using eq 7b, with values of $K_\mathrm{Cd\text{-}QD}$ from Table 1.

The presence of the coefficients θ and $(1 - \theta)$ in eq 3 implies a specific, probabilistic interpretation of the evolution of an exciton in a CdSe QD. These coefficients do not exist in the expression for the PL quantum yield of a molecular fluorophore ($\Phi = k_\mathrm{r}/(k_\mathrm{r} + k_\mathrm{nr})$) because, in the molecular case, the competition between radiative and nonradiative decay depends *only* on the relative magnitudes of k_r and k_nr. In colloidal QDs in the strong confinement regime, the molecular picture is not adequate to describe the fact that, although the core of the QD and the surface of the QD have very different properties, they are intimately coupled, and the exciton, although created in the core, will certainly couple to one or more surface states within its radiative lifetime.[9,11−21] The probability that the exciton will decay nonradiatively thus depends not only on the relative magnitudes of k_r and k_nr but also on the relative probabilities of the exciton interacting with a well-passivated surface site or a poorly passivated site, given by $(1 - \theta)$ and θ, respectively. The expression for quantum yield therefore must include $(1 - \theta)$ and θ as well as k_r and k_nr.

Inspection of the data in Table 2 yields four important observations: (i) In general, $k_\mathrm{nr} \gg k_\mathrm{r}$. If we approximate $(k_\mathrm{nr} - k_\mathrm{r})/k_\mathrm{r}$ as $k_\mathrm{nr}/k_\mathrm{r}$, then the nonradiative process is approximately a factor of 10^3 to 10^7 faster than the radiative process. This observation is reasonable considering that τ_r is on the order of tens to hundreds of nanoseconds for CdSe QDs,[40] and nonradiative processes with subpicosecond lifetimes have been observed in these systems.[72,73] (ii) The value of the fitting parameter, C, varies over 4 orders of magnitude. Both previous

(70) Young, A. G.; Green, D. P.; McQuillan, A. J. *Langmuir* **2006**, *22*, 11106–11112.
(71) Carrott, P. J. M.; Mourao, P. A. M.; Ribeiro Carrott, M. M. L.; Goncalves, E. M. *Langmuir* **2005**, *21*, 11863–11869.

measurements of $K_{Cd\text{-}ion}$[62] and our qualitative NMR analysis of $K_{Cd\text{-}QD}$ for the series R-An indicate that $K_{Cd\text{-}QD}$ does not vary over 4 orders of magnitude (but rather less than 1 order of magnitude). Our model, summarized in eq 7b, attributes the range in values of C to a range in values of k_{nr} over the series R-An. The observed dependence of PL quenching efficiency on R (Figure 2), therefore, is dominated by relative values of k_{nr} and not by their relative affinities for the surface, $K_{Cd\text{-}QD}$. (iii) The values of k_{nr}/k_r for $(Me)_2$N-An and MeO-An are higher than those for An, Br-An, and OCF_3-An. A plot of k_{nr}/k_r vs the Hammett coefficient, σ (Table 1), of R leads to a "V-shaped" plot, with a change in slope at $\sigma = 0$ (see Supporting Information); nonlinear Hammett plots of this shape usually indicate a change in mechanism for the process under investigation.[74] (iv) The values of n follow this same "V-shaped" trend as that for k_{nr}/k_r. The next sections assign a physical interpretation to these observations.

Mechanisms for Nonradiative Decay of the Exciton Include Trapping of the Electron and Photoinduced Hole Transfer. In the model for PL of the QD outlined above, k_{nr} is the rate of nonradiative decay of the exciton once it couples to a surface site occupied by an R-An ligand. Possible mechanisms for nonradiative decay include (i) transfer of energy (as a bound electron−hole pair), probably via a dipole−dipole mechanism, from the QD to the R-An ligand; (ii) transfer of a hole from the HOMO of the photoexcited QD to the HOMO of a ground-state R-An ligand (reductive quenching), Figure 4A; and (iii) trapping of the photoexcited electron in the antibonding orbital associated with the R-An:Cd^{2+} bond that is near or below the energy of the QD LUMO, Figure 3C. We can eliminate mechanism i, energy transfer, immediately for all of the R-An ligands because the lowest energy excited states of these ligands are at higher energies than the exciton of the QD.

To investigate mechanism ii, reductive quenching, we calculated the ionization potentials of the R-An molecules for free, gas-phase species using DFT (B3LYP, 6-311G**, see Supporting Information for details). Figure 4B shows these potentials and the HOMO and LUMO of a 2.7-nm QD, obtained by ultraviolet photoemission spectroscopy.[75] Both sets of potentials are shown relative to vacuum. The ionization potentials of An, Br-An, and OCF_3-An are >1 eV below the energy of the HOMO of the QD, so it is energetically unfeasible for these ligands, in their ground state, to donate an electron to the HOMO of a photoexcited QD. The resonance structures of $(Me)_2$N-An and MeO-An stabilize their radical cations and make these molecules significantly easier to oxidize than the other R-An ligands,[76,77] so it is possible that both $(Me)_2$N-An and MeO-An reductively quench the QD through hole transfer, Figure 4A. Sharma et al. observed hole transfer from CdSe QDs to *p*-phenylenediamine (a molecule similar to $(Me)_2$N-An).[34] Although it appears that hole transfer from the HOMO of the QD to the HOMO of MeO-An is energetically uphill, the probability that this reaction will occur increases on going from the gas-phase picture in Figure 4B to the experimental system because of the (a) stabilization of the charge-separated state by solvent, (b) increase in electronic coupling between the QD and the ligand upon coordination, and (c) decrease in the energy of the HOMO of the QD (due to decrease in the Coulombic repulsion between paired electrons) as it is depopulated by photoexcitation.

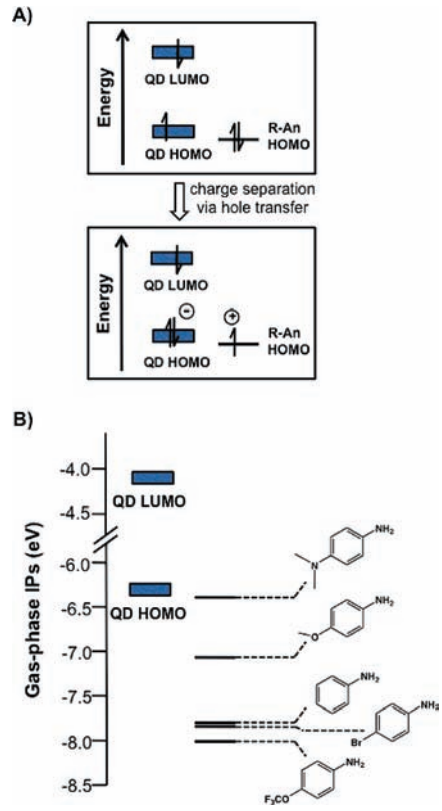

Figure 4. (A) Mechanism of photoinduced hole transfer from the HOMO of a photoexcited QD to the HOMO of R-An to form the radical pair $QD^{-\bullet}-(R\text{-}An)^{+\bullet}$. (B) Gas-phase HOMO and LUMO of a 2.7-nm QD, and gas phase ionization potentials (IPs) of R-An calculated with DFT (B3LYP, 6-311G**). The width of the HOMO and LUMO levels of the QD equal the fwhm of the first absorption peak of the QDs.

The ligands An, Br-An, and OCF_3-An probably decrease the PL of the QDs through mechanism iii, electron trapping, which involves the transfer of an electron from the LUMO of the photoexcited QD to the antibonding orbital of the R-An:Cd^{2+} bond. The position of the antibonding orbital depends on (a) the electronegativity of the electron-donating headgroup (the electronegativity of the amine increases as the basicity of the amine decreases),[78] and (b) the strength of the interaction between the lone pair of the amine and Cd^{2+}, which determines the magnitude of the splitting between bonding and antibonding orbitals upon coordination.[79] These effects determine the relative energies of the orbitals shown in the diagram in Figure 5.

Anilines with Electron-Donating Substituents Are Reductive Quenchers, and Anilines with Electron-Withdrawing Substituents Are Weak Passivators. In order to confirm that $(Me)_2$N-An and MeO-An act through reductive quenching, and An, Br-An, and OCF_3-An act through electron trapping, we split a single synthetic batch of CdSe QDs into two groups. The QDs in group

(72) Klimov, V. I. M., A. A.; McBranch, D. W.; Leatherdale, C. A.; Bawendi, M. G. *Phys. Rev. B* **2000**, *61*, R13349–R13352.
(73) Sewall, S. L.; Cooney, R. R.; Anderson, K. E. H.; Dias, E. A.; Kambhampati, P. *Phys. Rev. B* **2006**, *74*, 235328/1–235328/8.
(74) Isaacs, N. *Physical Organic Chemistry*, 2nd ed.; Pearson Education: New York, 1995.
(75) Carlson, B.; Leschkies, K.; Aydil, E. S.; Zhu, X.-Y. *J. Phys. Chem. C* **2008**, *112*, 8419–8423.
(76) Lauteslager, X. Y.; van Stokkum, H. M.; van Ramesdonk, H. J.; Bebelaar, D.; Fraanje, J.; Goubitz, K.; Schenk, H.; Brouwer, A. M.; Verhoeven, J. W. *Eur. J. Org. Chem.* **2001**, 3105–3118.
(77) Weiss, E. A.; Tauber, M. J.; Ratner, M. A.; Wasielewski, M. R. *J. Am. Chem. Soc.* **2005**, *127*, 6052–6061.
(78) Leung, L. K.; Meyer, G. J.; Lisensky, G. C.; Ellis, A. B. *J. Phys. Chem.* **1990**, *94*, 1214–1216.
(79) Scharlin, P. *Acta Chem. Scand.* **1986**, *40*, 207–209.

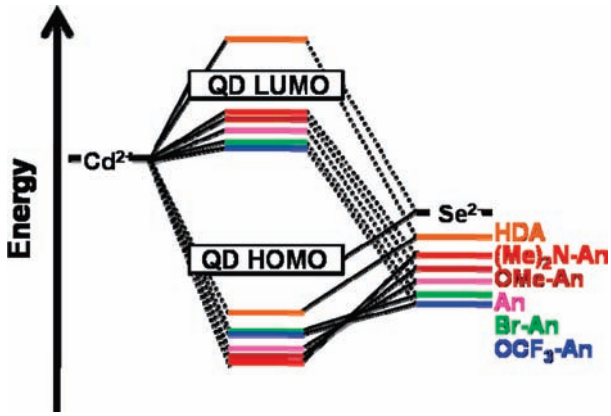

Figure 5. Predicted trend in the energies of the σ-donating orbitals of the R-An series. The energy splitting between bonding and antibonding orbitals of R-An:Cd^{2+} increases with increasing basicity of the lone pair. For reference, we include the position of HDA, which is a sufficiently strong σ-donor to eliminate the electron-trapping midgap state.

1 underwent the same purification procedure as those QDs studied to obtain the data in Figure 2. The QDs in group 2 underwent that procedure plus one extra precipitation from MeOH. Precipitation from MeOH pushes the equilibria of loosely bound native ligands toward the free, unbound state by reducing the concentration of excess free ligand in the dispersion and therefore reduces the equilibrium surface coverage of the QDs.[24] The Supporting Information contains ^{1}H NMR and ^{31}P NMR spectra that demonstrate the removal of excess free ligand on going from group 1 to group 2 QDs. The QDs in group 2 therefore have a larger number of initially unpassivated surface sites than do the QDs in group 1 at equilibrium. This decrease in surface coverage is reflected in the decrease in PL quantum yield on going from group 1 QDs to group 2 QDs: For ten batches of CdSe QDs of diameters ranging from 2.7 to 3.2 nm, the average PL quantum yield (measured using a Rhodamine 6G standard) is 20.3 $\pm$ 4.8% for those prepared identically to group 1 samples, and 11.8 $\pm$ 3.7% for those prepared identically to group 2 samples.

Figure 6A plots the PL/PL_0 of these two groups of QDs, shown in Figure 6B, after exposure to selected concentrations of each of the R-An ligands. The QDs used for this experiment (both group 1 and group 2) have slightly larger diameters (3.2 nm) than those of the QDs used to collect the data in Figure 2, so we do not expect that their PL at a given [R-An]:[QD] will necessarily match that in Figure 2. Inspection of Figure 6A reveals that the PL/PL_0 of QDs exposed to MeO-An and $(Me)_2$N-An ligands *decreases* as the number of the empty sites initially present on the surface increases. This result suggests that, if the exciton couples to a site coordinated to $(Me)_2$N-An or MeO-An, it is less likely to recombine radiatively than if it coordinates to a site with a bare Cd^{2+} ion; that is, $(Me)_2$N-An and MeO-An are active quenchers. These two ligands do passivate the surface state, but this passivation is negated by the participation of the ligands in a separate quenching mechanism (here, hole transfer). In contrast, the PL/PL_0 of QDs exposed to An, Br-An, and OCF_3-An ligands remains constant or even increases slightly as the number of empty sites on the QDs before ligand exchange increases.[80] This observation suggests that these three ligands are weak passivators: they

(80) The fact that PL/PL_0 for a given [R-An]:[QD] does not decrease for QDs with a higher density of empty sites also indicates that An, Br-An, and OCF_3-An do not create hole traps upon coordination.

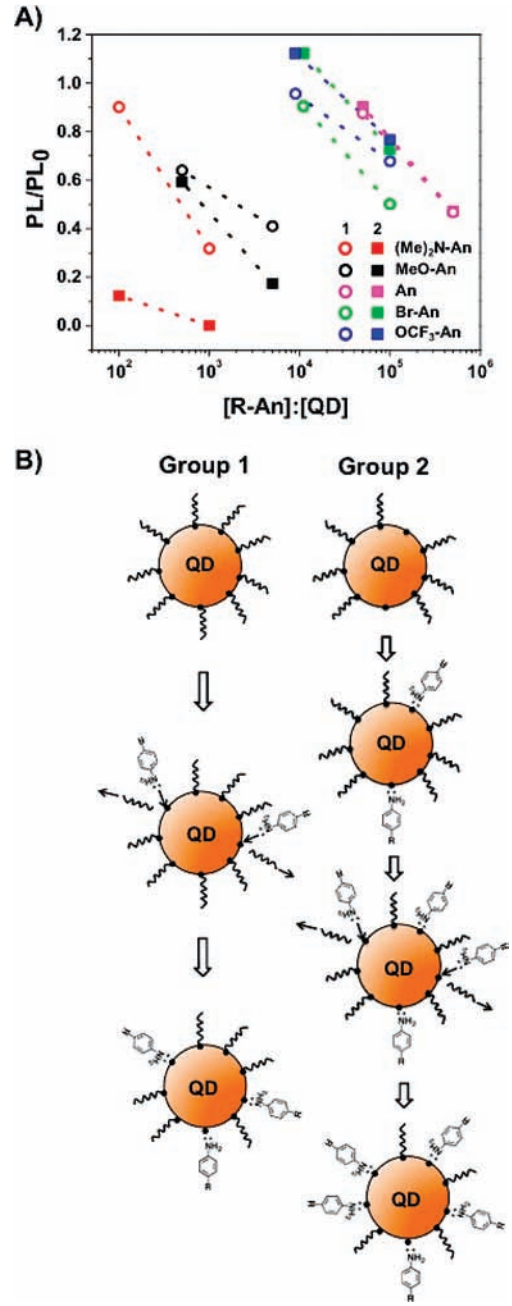

Figure 6. (A) PL/PL_0 plotted against [R-An]:[QD] for 3.2-nm QDs purified with one precipitation from MeOH (group 1, open circles), and QDs purified with two precipitations from MeOH (group 2, filled squares). Dotted lines are guides for the eye. The points with [Br-An]:[QD] = 10^4 and [OCF_3-An]:[QD] = 10^4 are offset horizontally for clarity. (B) Schematic description of the ligand exchange process for groups 1 and 2. Group 1 follows the two-state model for surface composition of the QDs used to derive eqs 3−7: before addition of R-An ligands, the surface is completely covered with native ligands. At some value of [R-An]:[QD] determined by $K_{Cd\text{-}QD}$, anilines begin displacing native ligands. For group 2, the R-An ligands first fill empty sites before displacing native ligands.

create antibonding orbitals with Cd^{2+} ions that have energy near or below the energy of the LUMO but above the energy of an empty Cd^{2+} site (Figure 5). As a point of reference, addition of HDA, a strong σ-donor and strong passivator (Figure 5), results in a PL/PL_0 of 1.3 for group 1, and 1.9 for group 2 ([HDA]:[QD] = 10^4). The fact that, upon going from group 1 QDs to group 2 QDs, PL/PL_0 changed in opposite directions for the proposed active quenchers and the proposed weak passivators

means that these effects were not merely due to an increase in the equilibrium population of R-An ligands on the surface postexchange (due to less competition from free native ligands in group 2 than in group 1), as shown in Figure 6B. If this difference in the equilibrium coverage of R-An were the primary determinant of the change in PL, we would observe a *consistent decrease* in PL/PL$_0$ on going from group 1 to group 2 QDs (at a constant value of [R-An]:[QD]) for *all* of the R-An ligands because fewer R-An ligands would be required to achieve the same decrease in PL.

The values of k_{nr} that we observe are then a result of two different mechanisms for nonradiative decay. The values of k_{nr} for $(Me)_2$N-An and MeO-An are dominated by the rate of hole transfer, and the values of k_{nr} for OCF_3-An, Br-An, and An are dominated by the rate of electron trapping. The observed trend in k_{nr} shows that the hole transfer process is faster than the electron trapping process for these systems. This observation is reasonable considering previously measured time constants for hole transfer (<1 ps for CdSe QD−pyridine complexes,[72] and 3 ps for CdSe−thiophenol complexes[81]) and for electron trapping (100−400 ps in small CdSe QDs).[11,73,82,83]

We can explain the trend $k_{nr}(OCF_3\text{-An}) > k_{nr}(Br\text{-An}) > k_{nr}(An)$ by describing the process of electron trapping as an electron transfer from the LUMO of the core of the QD to the antibonding orbital formed by coordination of the R-An ligand to Cd^{2+} [84] and modeling this electron transfer process with Marcus theory. Marcus theory[85,86] is a set of phenomenological equations that have successfully described heterogeneous[87,88] electron transfer reactions and have been used by Jones et al. to relate PL dynamics to trapping dynamics in CdSe/ZnS QDs.[40] Within the Marcus treatment, k_{nr} observes the proportionality in eq 8, where k_B is the

$$k_{nr} \propto \exp \frac{-(\Delta G - \lambda)^2}{4\lambda k_B T} \quad (8)$$

Boltzmann constant, T is temperature, ΔG is the change in free energy on going from the reactant state (where the electron is in the LUMO of the QD) to the product state (where the electron is in the antibonding orbital of the R-An:Cd^{2+} bond), and λ is the total energy required for the system (solvent plus inner-sphere modes) to reorganize to achieve the geometry for electron transfer.

Inspection of eq 8 reveals that, for reactions where $|\Delta G| < \lambda$, k_{nr} increases as $|\Delta G|$ increases—that is, as the reaction becomes more exothermic; this scenario is called the Marcus normal region. Jones et al.[40] estimate that $\lambda \sim 230$ meV for the trapping of electrons by surface states on 2.9-nm CdSe QDs in $CHCl_3$. Several experimental[89−93] studies have concluded that, in CdSe QDs, electrons are "shallowly trapped" on poorly passivated Cd^{2+} sites—that is, the energies of electron trap sites are near or slightly below (0−50 meV) the energy of the QD LUMO. These studies imply that $|\Delta G|_{trap} < \lambda$. The electron trapping reactions therefore fall in the Marcus normal region, so our observed trend, $k_{nr}(OCF_3\text{-An}) > k_{nr}(Br\text{-An}) > k_{nr}(An)$, occurs because $|\Delta G|_{trap}(OCF_3\text{-An}) > |\Delta G|_{trap}(Br\text{-An}) > |\Delta G|_{trap}(An)$ (Figure 5).

The physical interpretation of the values of the fitting parameter n is somewhat ambiguous, but we believe that this parameter reflects both (i) the degree to which the binding of one R-An ligand affects the probability of binding of another R-An ligand (either through electrostatic perturbation of the QD surface or steric hindrance)[70,71] and (ii) a contribution of the electronic interaction (via passivation or charge transfer) between the R-An ligand and the QD to the observed PL/PL$_0$ that is not accounted for by the factor $(k_{nr} - k_r)/k_r$. Unsubstituted aniline, which has a small, electronically inert substituent, $R = H$, has the smallest value of n, and OCF_3-An, which has a large, electronically active substituent has the largest value of n.

Summary and Conclusions

We found that the dependence of PL/PL$_0$ of solutions of CdSe QDs on the concentration of added para-subsituted anilines, R-An (Chart 1 and Figure 2), requires a model that incorporates a binding isotherm and a function that accounts for the magnitude of the rate constant for nonradiative decay of the exciton in the presence of the R-An ligands. We determined that PL/PL$_0$ depends on the substituent R through three major mechanisms: (i) R determines the binding affinity of the aniline ligand for the surface of the QD by controlling the steric and electronic availability of the lone pair on the nitrogen atom of the primary amine. (ii) R determines the σ-donating ability of the aniline and its ability to passivate a Cd^{2+} surface site (Figure 5). (iii) R determines the oxidation potential of the R-An ligand; this potential determines whether the R-An ligand can quench the PL by accepting a hole from the photoexcited QD (Figure 4).

We estimated the relative contributions of these mechanisms by calculating $K_{Cd\text{-}QD}$ using independent measurements of the metal−ligand binding constants, $K_{Cd\text{-}ion}$, and using eq 7b to predict the values of k_{nr}/k_r for the nonradiative decay process associated with each R-An. Previous measurements of $K_{Cd\text{-}ion}$[62] and our NMR analysis of $K_{Cd\text{-}QD}$ indicate that the response of PL/PL$_0$ to addition of R-An ligands is dominated by mechanisms ii and iii and not by the relative binding affinities of the R-An ligands, $K_{Cd\text{-}QD}$ (mechanism i). The relative values of k_{nr}/k_r for the series R-An strongly suggest that the series of R-An ligands separates into two groups: reductive quenchers ($(Me)_2$N-An and MeO-An) and weak passivators (An, Br-An, and OCF_3-An). Our observations that $(Me)_2$N-An and MeO-An decreased the PL of QDs upon binding to empty sites on the surface, and that An, Br-An, and OCF_3-An either did not change or increased the PL upon binding to empty sites (Figure 6) support this assertion.

(81) Burda, C.; Link, S.; Mohamed, M.; El-Sayed, M. *J. Phys. Chem. B* **2001**, *105*, 12286–12292.
(82) Sewall, S. L.; Cooney, R. R.; Anderson, K. E. H.; Dias, E. A.; Sagar, D. M.; Kambhampati, P. *J. Chem. Phys.* **2008**, *129*, 084701/1−084701/8.
(83) Klimov, V. I. *J. Phys. Chem. B* **2000**, *104*, 6112–6123.
(84) Aharoni, A. O., D.; Banin, U.; Rabani, E.; Jortner, J. *Phys. Rev. Lett.* **2008**, *100*, 057404/1−057404/4.
(85) Marcus, R. A. *J. Chem. Phys.* **1984**, *81*, 4494–4500.
(86) Marcus, R. A. *Rev. Mod. Phys.* **1993**, *65*, 599–610.
(87) She, C.; Anderson, N. A.; Guo, J.; Liu, F.; Goh, W.-H.; Chen, D.-T.; Mohler, D. L.; Tian, Z.-Q.; Hupp, J. T.; Lian, T. *J. Phys. Chem. B* **2005**, *109*, 19345–19355.
(88) Clifford, J. N.; Palomares, E.; Nazeeruddin, M. K.; Gratzel, M.; Nelson, J.; Li, X.; Long, N. J.; Durrant, J. R. *J. Am. Chem. Soc.* **2004**, *126*, 5225–5233.
(89) Nemec, P.; Maly, P. *J. Appl. Phys.* **2000**, *87*, 3342–3348.
(90) Trojanek, F.; Cingolani, R.; Cannoletta, D.; Mikes, D.; Nemec, P.; Uhlirova, E.; Rohovec, J.; Maly, P. *J. Cryst. Growth* **2000**, *209*, 695–700.
(91) Underwood, D. F.; Kippeny, T.; Rosenthal, S. J. *J. Phys. Chem. B* **2001**, *105*, 436–443.
(92) Lifshitz, E.; Dag, I.; Litvin, I.; Hodes, G.; Gorer, S.; Reisfeld, R.; Zelner, M.; Minti, H. *Chem. Phys. Lett.* **1998**, *288*, 188–196.
(93) Lifshitz, E.; Dag, I.; Litvitn, I. D.; Hodes, G. *J. Phys. Chem. B* **1998**, *102*, 9245–9250.

We recognize that the PL of a single QD can be partially quenched by creation of electron traps through modulation of the ratio of "on time" to "off time" in the PL blinking characteristics of the QDs. Munro et al.[25] observed modulation of blinking statistics in single-QD PL measurements of QDs exposed to hole-trapping thiol ligands. This mechanism is also compatible with our model in that the progressive displacement of native ligands by R-An ligands results in a continuous increase in the "off time" relative to the "on time" for each QD and therefore a continuous decrease in the observed steady-state PL of the sample. The larger the value of k_{nr} for a given R-An ligand, the steeper the increase of "off time" with increasing displacement of native ligands.

This study underscores the dramatic sensitivity of the optical properties of QDs to their surface chemistry, and the great potential that exists to tune these properties by rationally designing organic ligands. We are currently performing time-resolved absorption and PL measurements on the R-An:QD systems in order to measure the time constants for decay of the exciton and to confirm the presence of charge transfer for the QDs coordinated to $(Me)_2$N-An and MeO-An. Because the exciton lifetime decays multiexponentially in CdSe systems, a kinetic model is necessary in addition to these measurements to determine k_{nr} and k_r. The values of the rate constants that we predicted from steady-state PL measurements in this work, and the mechanistic predictions that the rate constants yield, will assist us in interpreting the results of the time-resolved experiments. We are also currently developing experiments to measure directly the binding constants of R-An ligands with QDs through temperature-dependent NMR.

Acknowledgment. We acknowledge funding from the Camille and Henry Dreyfus Foundation through the Dreyfus New Faculty award, the Henry Luce Foundation, and the MURI/DURINT program of the DoD.

Supporting Information Available: Details of the synthesis of CdSe QDs, discussions of the Langmuir model, details of the DFT calculations, and Figures S1−S10 showing a histogram of the size distribution of QDs from TEM, the time-dependence of the PL response to exposure to R-An ligands, ^{1}H NMR spectra of the free R-An ligands, the plot of $K_{Cd\text{-}ion}$ versus Hammett coefficients, ^{1}H NMR analysis of the binding constants of the R-An ligands to the QDs, spin-density distributions for the radical cations of the R-An ligands, DFT-calculated geometries of the R-An ligands, plots of PL/PL_0 vs [R-An], the plot of $(k_{nr}\text{-}k_r)/k_r$ vs Hammett coefficient, and NMR spectra of group 1 and group 2 QD−ligand dispersions. This material is available free of charge via the Internet at http://pubs.acs.org.

JA907253S